Journal of Biomedical Optics

BiomedicalOptics.SPIEDigitalLibrary.org

In vivo performance of a visible wavelength optical sensor for monitoring intestinal perfusion and oxygenation

Mitchell B. Robinson
Anna M. Wisniowiecki
Ryan J. Butcher
Mark A. Wilson
M. Nance Ericson
Gerard L. Cote

SPIE.

Mitchell B. Robinson, Anna M. Wisniowiecki, Ryan J. Butcher, Mark A. Wilson, M. Nance Ericson, Gerard L. Cote, "*In vivo* performance of a visible wavelength optical sensor for monitoring intestinal perfusion and oxygenation," *J. Biomed. Opt.* **23**(5), 055004 (2018), doi: 10.1117/1.JBO.23.5.055004.

In vivo performance of a visible wavelength optical sensor for monitoring intestinal perfusion and oxygenation

Mitchell B. Robinson,[a] Anna M. Wisniowiecki,[a] Ryan J. Butcher,[a] Mark A. Wilson,[b,c] M. Nance Ericson,[d] and Gerard L. Cote[a,e,*]
[a]Texas A&M University, Optical Biosensing Laboratory, Department of Biomedical Engineering, College Station, Texas, United States
[b]VA Pittsburgh Healthcare System, Pittsburgh, Pennsylvania, United States
[c]University of Pittsburgh, Department of Surgery, Pittsburgh, Pennsylvania, United States
[d]Consultant, Knoxville, Tennessee United States
[e]TEES Center for Remote Healthcare Technologies and Systems, College Station, Texas, United States

Abstract. Traumatic injury resulting in hemorrhage is a prevalent cause of death worldwide. The current standard of care for trauma patients is to restore hemostasis by controlling bleeding and administering intravenous volume resuscitation. Adequate resuscitation to restore tissue blood flow and oxygenation is critical within the first hours following admission to assess severity and avoid complications. However, current clinical methods for guiding resuscitation are not sensitive or specific enough to adequately understand the patient condition. To better address the shortcomings of the current methods, an approach to monitor intestinal perfusion and oxygenation using a multiwavelength (470, 560, and 630 nm) optical sensor has been developed based on photoplethysmography and reflectance spectroscopy. Specifically, two sensors were developed using three wavelengths to measure relative changes in the small intestine. Using vessel occlusion, systemic changes in oxygenation input, and induction of hemorrhagic shock, the capabilities and sensitivity of the sensor were explored *in vivo*. Pulsatile and nonpulsatile components of the red, blue, and green wavelength signals were analyzed for all three protocols (occlusion, systemic oxygenation changes, and shock) and were shown to differentiate perfusion and oxygenation changes in the jejunum. The blue and green signals produced better correlation to perfusion changes during occlusion and shock, while the red and blue signals, using a new correlation algorithm, produced better data for assessing changes in oxygenation induced both systemically and locally during shock. The conventional modulation ratio method was found to be an ineffective measure of oxygenation in the intestine due to noise and an algorithm was developed based on the Pearson correlation coefficient. The method utilized the difference in phase between two different wavelength signals to assess oxygen content. A combination of measures from the three wavelengths provided verification of oxygenation and perfusion states, and showed promise for the development of a clinical monitor. [DOI: 10.1117/1.JBO.23.5.055004]

Keywords: spectroscopy; perfusion; oxygenation; hemorrhage; shock.

Paper 180019RR received Jan. 11, 2018; accepted for publication Apr. 26, 2018; published online May 18, 2018.

1 Introduction

Percentages of "preventable" United States civilian and military trauma-related deaths involving hemorrhage are greater than 16% and 66%, respectively.[1] More than 90% of deaths due to hemorrhage occur within the first 6 h of hospital admission, making resuscitation strategy critical.[2] The primary goal and the current standard of care for trauma patients is to restore tissue oxygenation by controlling bleeding and administering intravenous volume resuscitation before addressing secondary injuries.[3,4] Adequate resuscitation to restore tissue blood flow and oxygenation is critical within the first hours following admission.[2] Current clinical methods for guiding resuscitation lack the required sensitivity and specificity to assure adequate treatment while avoiding complications associated with inadvertent overtreatment. To better address these issues, an approach was developed for monitoring intestinal perfusion and oxygenation *in vivo* using a prototype, multiwavelength optical sensor based on photoplethysmography (PPG) and reflectance spectroscopy.

Abdominal injuries are often associated with significant hemorrhagic shock and typically require early operation for control of bleeding. In such cases, surgical intervention is divided into a primary operation to control bleeding followed by resuscitation and a repeat operation within 48 h to address secondary injuries. This staged clinical process permits access to the small intestine for monitoring tissue perfusion and oxygenation during hemorrhagic shock resuscitation. Between primary and secondary surgical operations, intestinal monitoring can be accomplished during the primary intervention by introducing a short-term implantable monitor. Furthermore, removal of the monitor can then occur during the secondary intervention.

Impairment of the microcirculation occurs during hemorrhagic shock and continues for up to 72 h even if one controls the bleeding.[5] This condition is characterized by decreased tissue perfusion and tissue oxygen deficits, which leads to tissue

*Address all correspondence to: Gerard L. Cote, E-mail: gcote@tamu.edu

1083-3668/2018/$25.00 © 2018 SPIE

injury. Inadequate resuscitation of shock patients can also contribute to further tissue ischemia and a condition called multiple organ dysfunction syndrome (MODS), which is the leading cause of death in surgical intensive care units.[6] Hemorrhage and insufficient resuscitation expose certain organs, especially the intestines, to states of low perfusion and reduced oxygenation, resulting in worsening tissue acidosis, oxygen debt, and the potential for cellular necrosis, which contribute to MODS. Alternatively, over-resuscitation may result in complications from edema.[7] Optimal patient resuscitation facilitates more prompt resolution of oxygen debt and limits the extent of tissue damage. Determination of optimal resuscitation is not formulaic and must be individualized, but is highly dependent upon the availability of intimate, real-time measures of patient physiology that reflect organ-specific tissue oxygenation.

Resuscitation, especially following initial control of hemorrhage, is often guided by systemic parameters, such as blood pressure and urine output, as surrogate markers for tissue ischemia or tissue perfusion. Systemic indicators, however, may not adequately detect the severity of tissue acidosis, remaining oxygen debt, and insufficient organ perfusion due to physiological compensatory responses. In particular, systemic blood pressure and oxygen saturation have been found to lack the necessary sensitivity[8,9] for adequate hemorrhagic shock resuscitation. Despite normalization of systemic indicators, a state of compensated shock develops in 85% of patients.[4] Therefore, more definitive metrics of microvascular dysfunction and tissue ischemia are needed to guide shock resuscitation. Clinically ideal markers of tissue oxygen deficit during the initial management of trauma patients in hemorrhagic shock have been elusive. Although poor outcomes have been correlated with low central venous oxygen saturation, arterial blood lactate elevation, and decreased serum base excess at the time of hospital admission,[10–12] these markers reflect whole-body oxygen deficit and may change too slowly compared to local measurements of tissue oxygenation[13] to guide resuscitation. Invasive and noninvasive measurements of blood pressure, coagulation, metabolism, and muscle oxygenation are used clinically to predict the severity and outcome of shock. However, the value of these strategies to guide resuscitation is less clear. Some cannot be measured rapidly; others are too complex for a bedside assay. Biomarkers from gastrointestinal (GI) mucosa, such as mucosal pH, are particularly useful because perfusion and oxygenation of these tissues are compromised to a greater extent during hemorrhage. Previous studies have shown that perfusion of the small intestine is one of the most sensitive indicators of shock.[14] Such organs lose blood flow first and are reperfused last.[9] However, previously explored measures have not achieved the necessary sensitivity, reliability, or general applicability[1,9] to be effective guides for resuscitation. An ideal measure of physiologic response to resuscitation from hemorrhagic shock would be rapid, repeatable over a short time interval, and sensitive.

Direct measurements of tissue perfusion, tissue acidosis, or oxygen consumption are better guides for resuscitation progress and the development of MODS.[15] In addition, microvascular blood flow and tissue oxygenation are closely related to tissue health.[16] To assess the efficacy of resuscitation in hemorrhagic shock patients, monitoring of local and peripheral tissue perfusion and oxygen consumption is ideal. Optical measurement of peripheral muscle oxygenation using visible and near infrared optical spectroscopy has been demonstrated as an early predictor of shock severity.[8,13,17] While the study concluded that mild, moderate, and severe shock could be detected and were statistically different from healthy patients, mild shock could not be differentiated from moderate shock. Peripheral muscle oxygenation is also used by some centers to guide resuscitation.[13]

Optical techniques are well suited to monitoring local tissue hemodynamics and are noninvasive to the tissue of interest. Optical spectroscopy using red to near-infrared (NIR) wavelengths is the gold standard for noninvasive quantification of hemoglobin oxygen saturation. The technique utilizes a pair of wavelengths, chosen, respectively, between 600 and 700 nm and 900 and 1000 nm.[18,19] Conventional devices are designed for denser tissues, such as skeletal muscle, the liver, the finger, and the brain, with median source–detector separations of 5 to 7 mm.[20,21] In the design of optical pulse oximeters and heart rate monitors, signal quality may be improved for specific applications through proper wavelength selection and source-to-detector separations.[22] In the case of intestinal monitoring, conventional NIR designs yield a poor signal-to-noise (SNR) ratio, as the intestinal wall is relatively thin (~2 mm)[23] and NIR wavelengths probe beyond the intestinal wall into the intestinal lumen and adjacent organs. This leads to high background noise and motion artifact in the detected signal.[24] In addition, reduced vascular density in the intestine and low hemoglobin signature using NIR wavelengths[25] result in an overall information-poor signal.

Taking advantage of visible wavelengths and short source-to-detector separations, a photoplethysmographic sensor has been designed, built, and validated *in vitro* to separate perfusion and oxygenation information acquired from the intestinal wall.[22,26] The use of visible wavelengths, with the increased scattering associated with shorter wavelengths and the increased absorbance of hemoglobin, confines photons within the perfused tissue and increases the hemoglobin signature in the collected optical signal. It is hypothesized that this sensor may be used to directly inform the physician on the resuscitation status via intestinal perfusion and oxygenation. In this study, the sensitivity of blue (470 nm), green (560 nm), and red (630 nm) wavelength photonic sensors was compared in an *in vivo* model of hemorrhagic shock for the measurement of intestinal perfusion and oxygenation.

2 Methods and Materials

2.1 *Animal Study Protocol*

Three New Zealand White rabbits were used in this study under animal use protocol AUP#2015-0001 approved by the Institutional Animal Care and Use Committee at Texas A&M University. Each animal was fasted from food for 12 h to avoid postprandial hyperemia of the intestine but was allowed *ad libitum* access to water. For each surgical procedure, animals were premedicated with 5 mg/kg xylazine IM and 25 mg/kg ketamine IM. Animals were placed on a heating pad and brought into the operating room. Anesthetic induction was completed with isoflurane at 3.5% with a flow rate of 1.5 L/min. Endotracheal intubation was performed and mechanical ventilation implemented to support respiration. Isoflurane was titrated to lower percentages to maintain adequate anesthetization. The abdomen was clipped and prepped with 2% CHG in alcohol. A femoral arterial catheter was inserted percutaneously and connected to a transducer for blood pressure monitoring and arterial blood sampling. Blood pressure and heart rate, peripheral pulse

oximetry, and end-tidal carbon dioxide were monitored. The femoral vein was cannulated for blood withdrawal during hemorrhagic shock, and percutaneous catheters in ear veins were used for maintenance of intravenous fluid administration. A midline laparotomy was performed to expose the small intestine, and a transonic transit-time ultrasound probe (Transonic Systems Inc., 2.5PSB) was placed on the cranial mesenteric artery to monitor changes of arterial flow to the small intestine. Proximal to the transonic flow probe, a balloon occluder was placed around the cranial mesenteric artery to alter regional blood flow without modifying the systemic blood pressure. Two of our custom optical sensors, prepared specifically for this study, were attached to the serosal surface of the small intestine with an intervening distance of 3 cm and were secured using 5/0 polypropylene sutures. The abdominal wall was closed without creating pressure on the sensors or intestines. The sensors were used to compare the efficacy of different wavelength combinations for discriminating changes in oxygenation from changes in perfusion by using separate protocols. The protocols designed to assess the sensor performance included regional reduction of arterial flow, hemorrhagic shock, and brief periods of systemic hypoxia with increased nitrogen concentration in inspired gases. Throughout the experiments, vital signs (body temperature, SpO_2, heart rate, blood pressure, etc.) were monitored and continuously recorded. A schematic of the custom and commercial equipment used in the study is shown in Fig. 1(a). Measurements were obtained for each optical sensor for all three protocols. At the end of the experiments, while the animal was still anesthetized, euthanasia was performed with a barbiturate derivative solution administered intravenously (80 to 120 mg/kg). The rabbits are referred to as 1 to 3. Due to the duration and complexity of physiological interventions, each rabbit was prioritized for two of the experimental protocols.

2.1.1 *Intestinal perfusion*

An inflatable vascular occluder (Harvard Apparatus, part # PY2 62-0110) was positioned on the cranial mesenteric artery proximal to the intestine and inflated in graded increments to partially and then completely occlude the vessel. Data were continuously

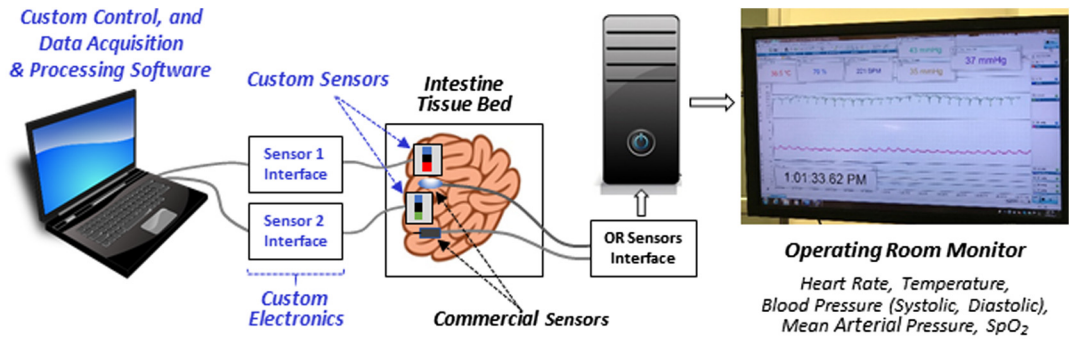

(a)

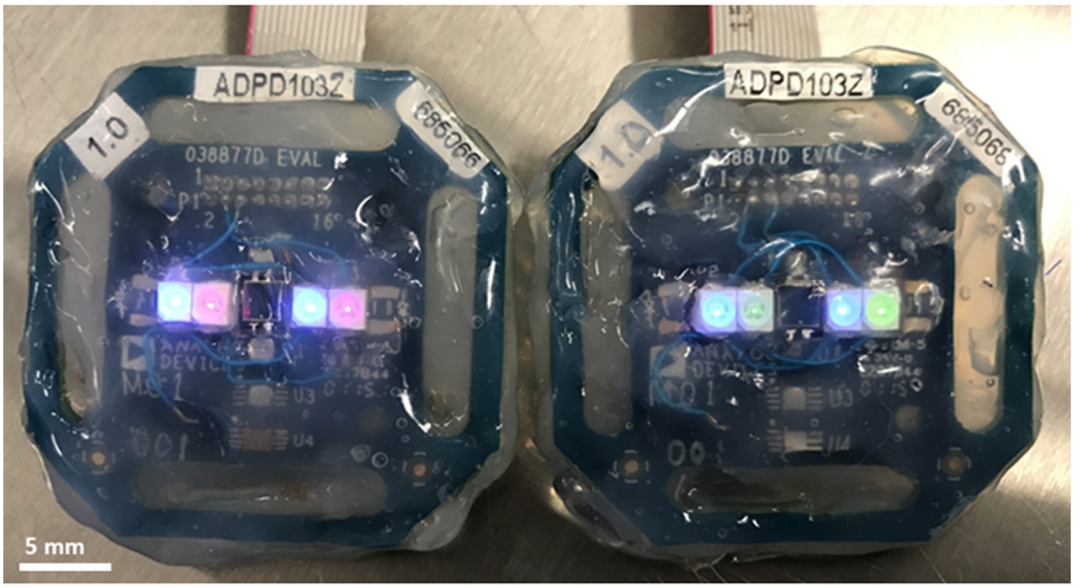

(b)

Fig. 1 (a) Systems diagram showing custom sensors sutured to the exterior of the small intestine at the jejunum, at separate locations. The corresponding signals were acquired using custom hardware and processed with software, as described in Sec. 2.4. Commercial sensors (transit-time flowmeter, arterial catheter, and SpO2 monitor) were placed on the cranial mesenteric artery and tongue (not pictured). Standard operating room (OR) equipment was used to monitor systemic vital signs. (b) The optical sensors used to probe the intestine are shown illuminating at operating intensity. The 470/630 nm sensor can be seen on the left and the 470/560 nm sensor can be seen on the right.

collected throughout the procedure. Following each increase in inflation, measurements were continued for 1 min. The process was repeated until the transit-time ultrasonic probe documented no flow, after which the inflator was depressurized, and flow was allowed to recover for 5 min. This procedure was repeated five times for each of the three animals.

2.1.2 *Oxygenation*

Blood oxygenation was altered by changing inhaled oxygen concentration with nitrogen blending (OxyDial™). Beginning at 22% inhaled oxygen, the inhaled concentration of oxygen was decreased by 1% every 5 min until systemic oxygen saturation fell to 80%, the lower limit specified in the AUP. This procedure was performed in rabbits 1 and 2.

2.1.3 *Hemorrhagic shock*

For this study, a fixed pressure model for hemorrhagic shock was used to produce desired changes in perfusion and tissue oxygenation. Hemorrhagic shock was induced by the removal of blood through a catheter in the femoral vein. Blood was removed until the mean arterial pressure reached 50% of its initial value (60 to 70 mmHg). Mean arterial pressure was maintained at the reduced value for 15 min with continued withdrawal of blood. After the 15-min hemorrhagic shock period, shed blood was returned over 5 min, and a volume of saline equal to two times the removed blood volume was infused, consistent with current shock resuscitation protocols.[27] This procedure was performed in rabbits 1 and 3.

2.2 *Optical Perfusion and Oxygenation Monitors*

Two optical sensors were sutured to the outer wall of the jejunum and operated in reflectance mode. The sensor boards utilized were modified ADPD103Z boards from Analog Devices.[26] As mentioned above, conventional optical perfusion and oxygenation measurements utilize long visible and NIR wavelengths, which enable increased penetration depth for dense tissues. For the thin intestinal tissues, the photon penetration is too deep at these long wavelengths, resulting in high background signals and motion artifact. Therefore, an isobestic visible wavelength (560 nm) and visible wavelengths (470 and 630 nm) on either side of the isobestic wavelength were chosen to enable sensitive perfusion and oxygenation measurement in the intestine. The reconfigured sensor boards for both the blue/green (470/560 nm) and blue/red (470/630 nm) LED configurations are depicted in Fig. 1(b). For a given LED wavelength pair, one LED of each wavelength was placed at the minimum 2 mm distance on either side of the centrally located photodetector. The second LED of each wavelength was placed on the opposite outside location resulting in a minimum spacing of 6 mm from the photodetector. The boards were then coated in electronics grade silicone (GC Electronics 19–160) to protect them from the abdominal environment. Measurements from the sensors were collected through the ADPD evaluation platform interface (Analog Devices, Massachusetts) and analyzed using MATLAB (Mathworks, Massachusetts). Comparisons of the wavelengths were performed using the signals collected by a single sensor board to ensure the analysis was restricted to the volumes of tissue being examined by each sensor.

2.3 *In-Vitro Verification*

An optofluidic tissue phantom was developed to mimic the optical properties and morphology of small intestinal tissue.[24,28] A blood phantom was also developed to mimic the optical properties of blood at the wavelengths of interest. A Vici-Valco M6 pump using an interface developed in LabVIEW (National Instruments) was used to flow the phantom blood through the tissue phantom. To examine differences in phase, a pulsed signal was input and the optical sensors were placed on the phantom to collect the PPG signal. Alterations to the optical properties of the blood phantom were introduced through the addition of aluminum oxide particles with a mean size less than 10 μm at a concentration of 20 mg/mL (SIGMA). Flow rates were increased by 0.2 mL/min for 5 min, reaching a maximum flow rate of 1 mL/min.

2.4 *Data Processing*

Pulsatile and nonpulsatile components of the signals were separated through adaptive filtering over segments of the signal, dependent upon the protocol being performed. Occlusion episodes were segmented using the steps in the occluder inflation. Hypoxia and shock episodes were segmented in 1-min time intervals. To maintain both magnitude and phase information contained in the pulsatile component of the signal, a peak-to-peak averaging process was performed. Each peak-to-peak interval was extracted and averaged giving an average beat waveform for that segment of the signal. Nonpulsatile components of the signal were extracted using a low pass filter from 0 to 0.1 Hz.

Perfusion index, PI, and modulation ratio, R, were calculated for each wavelength and each pair of wavelengths, respectively, on the two sensors using Eqs. (1) and (2):[29,30]

$$\mathrm{PI}_\lambda = \frac{\mathrm{AC}_\lambda}{\mathrm{DC}_\lambda}, \tag{1}$$

$$R = \frac{\mathrm{PI}_{\lambda_1}}{\mathrm{PI}_{\lambda_2}}, \tag{2}$$

where PI_λ is the PI for a particular wavelength, AC_λ is the magnitude of the pulsatile component of the signal, DC_λ is the magnitude of the nonpulsatile component of the signal, and R is the modulation ratio of the perfusion indices for the two different wavelengths. Traditional pulse oximetry uses the modulation ratio to calculate the oxygen saturation (SpO_2) of hemoglobin.[31] Given by Eq. (3), this four-parameter function is empirically fit to estimate the changes in oxygenation:

$$\mathrm{SpO}_2 = \frac{a - b \cdot R}{c - d \cdot R}, \tag{3}$$

where a, b, c, and d are, respectively: a, the absorption coefficient for the deoxygenated hemoglobin signal at wavelength one, b, the absorption coefficient for the deoxygenated signal at wavelength two times the ratio of the path lengths at wavelength two over wavelength one, c, the difference between deoxygenated and oxygenated absorption coefficients at wavelength one and, d, the difference between the oxygenated and deoxygenated absorption coefficient at wavelength two times the ratio of the path lengths at wavelength two over wavelength

one. Note that most pulse oximeters assume that the ratio of the path lengths for the two wavelengths to be constant (i.e., independent of inter-subject variability in the circulatory system). In this case, the coefficients, a through d, are constants and SpO_2 can be derived from R and these calibrated coefficients.

Estimations of changes in the primary source of signal generation between wavelengths were determined using the Pearson correlation coefficient based on findings discussed in Sec. 3. The Pearson correlation coefficient is given by Eq. (4):

$$r=\frac{n\sum(x_{\lambda_1}\cdot x_{\lambda_2})-\sum x_{\lambda_1}\cdot\sum x_{\lambda_2}}{\sqrt{\left[n\sum(x_{\lambda_1})^2-\left(\sum x_{\lambda_1}\right)^2\right]\cdot\left[n\sum(x_{\lambda_2})^2-\left(\sum x_{\lambda_2}\right)^2\right]}}, \tag{4}$$

where x denotes the array of values representing the averaged pulsatile waveform for the two wavelengths present on each of the sensors, n is the number of values in the array, and r is the Pearson correlation coefficient. The equation gives a measure of the linear correlation between two variables, $x_{\lambda 1}$ and $x_{\lambda 2}$. This coefficient has a value between $+1$ and -1, where $+1$ is total positive linear correlation, 0 is no linear correlation, and -1 is total negative linear correlation.

3 Results and Discussion

3.1 *Perfusion*

Changes in intestinal perfusion due to occlusion are seen in both the pulsatile and nonpulsatile components of the signals (Fig. 2). The error bars represent the standard deviation across all three rabbits for all five occlusion sequences performed in each of the rabbits.

As depicted in Fig. 2(b), the pulsatile component for all three wavelengths showed a reduced amplitude with occlusion. The red (630 nm) pulsatile signal can be seen to suffer from greater variability and has less dynamic range with full occlusion. The difference in absorption of light by oxygenated hemoglobin, with an absorption coefficient approximately two orders of magnitude lower at 630 nm than at 470 or 560 nm,[25] contributes to the noisier signal. The blue and green signals exhibit an average SNR of 25.7 and 15.6 dB, respectively, as compared to the red signal, which has an SNR of 0.89 dB in the oxygenated case and 14.8 dB in the deoxygenated case. SNR does not vary significantly for the blue and green signals between oxygenations. This change in SNR happens as a function of the increased penetration depth, as well as the reduced absorption of light in the red signal when the blood is oxygenated. This yields less signal to background at the red wavelength relative to the blue and green, as noted previously.[22] For the nonpulsatile component of the signal, the red wavelength shows a decrease in its signal with decreased flow, while, for the shorter blue (470 nm) and green (560 nm) wavelengths, reduced blood flow results in an increase in the nonpulsatile component of the signal. The framework that is used to process these signals and calculate the modulation ratio assumes that the change in nonpulsatile and pulsatile signal amplitude is due to changes in the absorption of the tissue, which, in the model framework, corresponds to changes in tissue perfusion.[31] The difference seen in the nonpulsatile signal intensity between wavelengths does not agree with this framework but is backed up by the literature. Specifically, both increases and decreases in the PPG signal with changes in the perfusion have been documented previously *in vivo* and *in vitro* in transmission and reflectance modes for capillary and large vessels.[32,33] The differences in signal response with wavelength have been attributed to a difference in the optical properties of the tissue being probed, as well as the placement of the sensor. Additional theories on the source of the PPG signal have been proposed,[34,35] including changes in the pressure in the vessel and compressing the tissue to alter

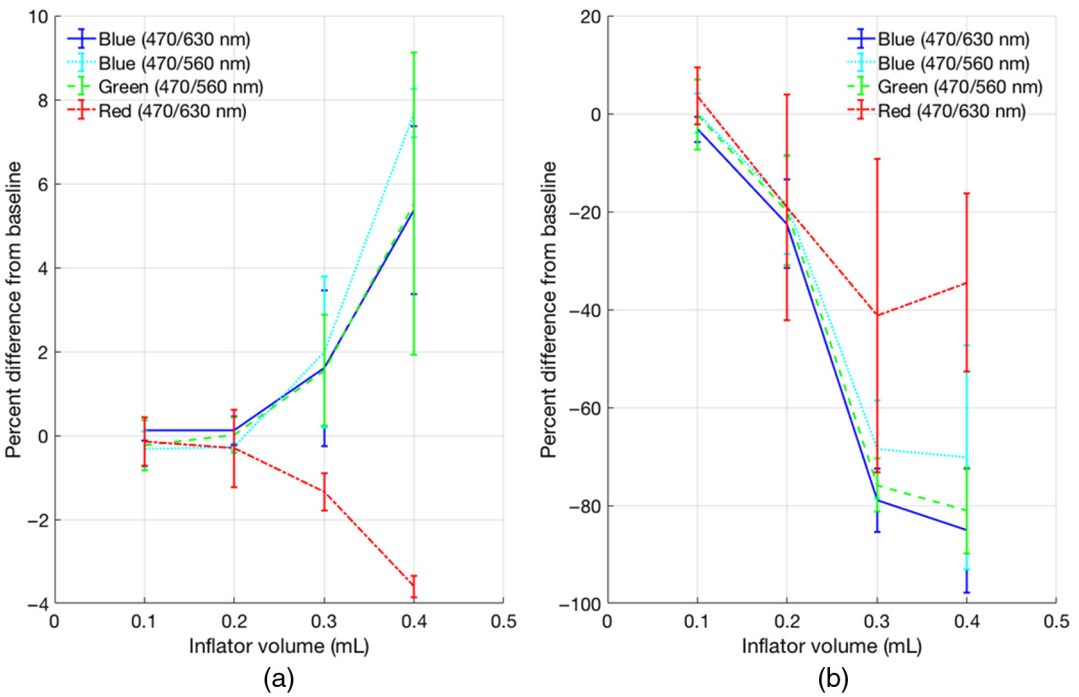

Fig. 2 Comparison of the signal changes in the (a) nonpulsatile component and (b) pulsatile component in response to the graded occlusions.

scattering properties. These theories focus on the interaction of the vasculature within skin, which is morphologically and optically different from vasculature in the intestine.[24] For the wavelengths studied, compared to the small intestine, the skin exhibits higher absorbance with comparable scattering, effectively limiting the light returning to the detector from traveling beyond a depth of 1 mm.[34] The reduced absorbance of the intestinal tissue results in an increased probing depth for the visible wavelengths as compared to skin, better enabling light to reach the pulsatile vessels in the tissue.[24] Here, we propose that two differing sources of signal generation are observed: the attenuation of light by absorbers in the blood tissue (in this case hemoglobin) and an increased reflectance. The reflectance changes are caused by alterations in the optical scattering property of the blood in the vessels due to oriented erythrocytes during increased flow rates[33] and changes in the distance from the vascular wall to the detector. For the bands of the hemoglobin spectra,[25] where absorbance is high as compared to scattering (blue and green wavelengths), absorbance dominates the signal generation. This is observed as decreased signal attenuation with decreased blood flow. Absorbance by oxygenated hemoglobin at 630 nm is relatively low compared to scattering, causing the primary signal generation to come from the change in the scattering property of the blood in the vessels and the magnitude of vascular expansion. The decrease in nonpulsatile signal intensity for the red signal results from the decrease in blood velocity, reducing both the alignment of the orientation of the red blood cells that increase reflected light as well as the expansion of the vessels.

The effects seen with wavelength *in vivo* were also validated using the previously described optofluidic phantom[26] by altering the scattering properties of the blood phantom used. Comparing the blood phantom to the same phantom with the addition of aluminum oxide particles with an increasing flow rate yielded the signals in Fig. 3. As depicted, the change in the scattering properties of the blood phantom impacted the nonpulsatile signal changes in ways similar to those seen *in vivo*. Increases in the red signal were observed when flow was increased and a scattering blood phantom was used. While orientation effects of the aluminum particles play less of a role, since the aluminum particles are of more consistent shape, the increase in the scattering properties of the blood phantom is similar to those *in vivo*. Here, it can be seen that the magnitude of the effect, whether a positive or negative trend is observed, is affected by the ratio of the absorption and scattering properties of the blood at the different wavelengths. With a greatly decreased absorption coefficient at the red wavelength,[25] the scattering effects are seen to dominate and result in increased detected signal with increased flow. The changes from baseline are smaller in magnitude in the *in vitro* case, with the greatest change overall not exceeding 1.5%. This is due to the phantom's vascular layer, which represents a single layer of vessels and is therefore less densely packed compared to the vascular bed explored *in vivo*. In addition, the dynamic range of flow rates explored with the phantom was smaller than those seen *in vivo*.

This difference in signal with wavelength for the nonpulsatile component can also be observed in the pulsatile component of the signals. With transient increases in flow due to the contraction of the heart, the effects giving rise to the changes in the nonpulsatile signal (orientation of cells and volumetric expansion of vessels) are observed in the pulsatile component of the signal as phase differences between the signals. Plotting the averaged pulsatile waveforms of the *in vivo* signals against each other shows the difference in the time course of the signal

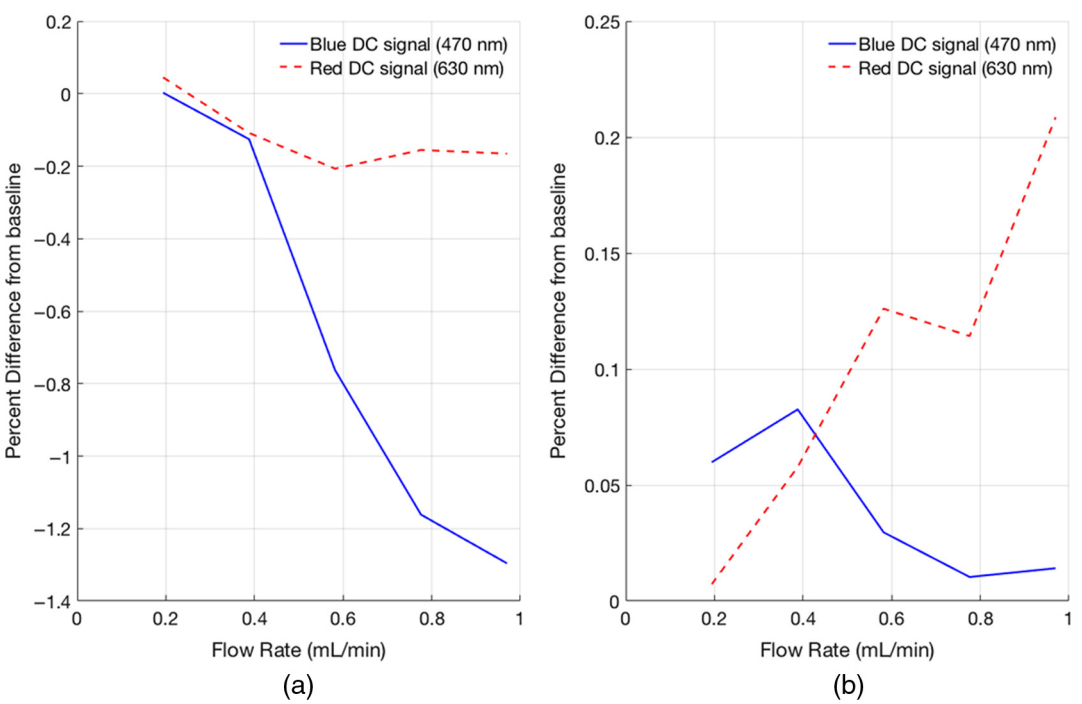

Fig. 3 Changes in nonpulsatile signal intensity measured in an optofluidic intestinal phantom in response to changes in flow rate for (a) absorption dominated blood phantom, as compared to (b) the same blood phantom with the addition of scattering particles. The general trend of increased flow leading to decreased signal is preserved in the absorbing case, but, upon addition of the scattering particles, the trend is reduced in the blue wavelength and opposite for the red wavelength.

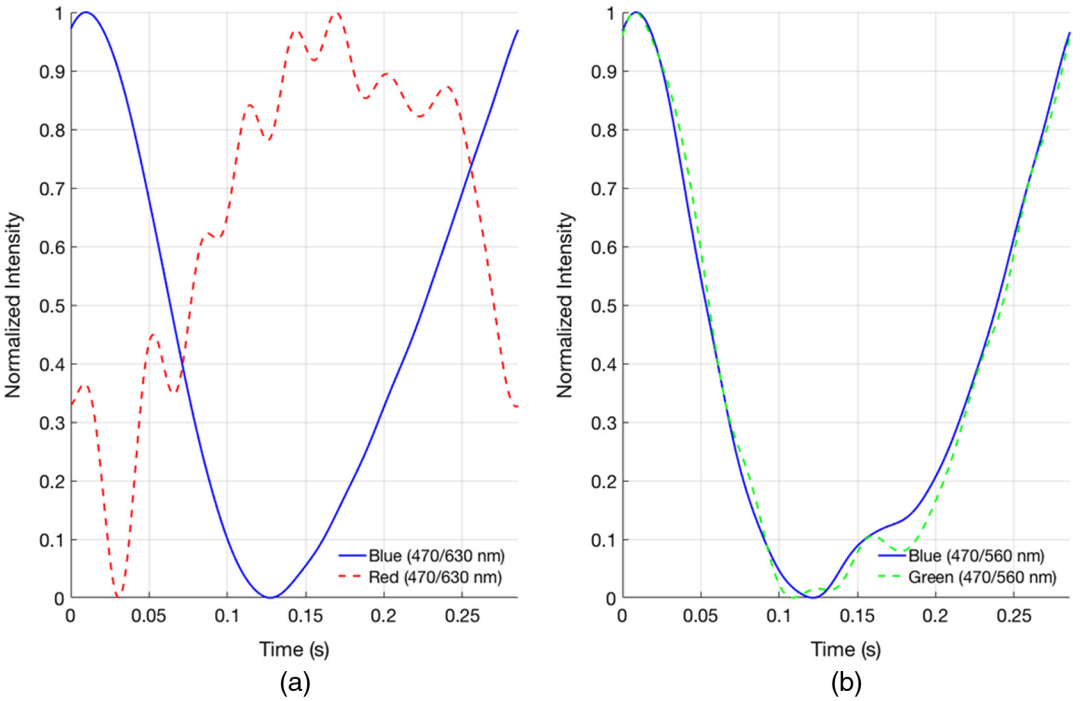

Fig. 4 Comparison of the pulsatile waveforms for the different wavelengths *in vivo*. (a) The difference in timing of the peak, as well as the morphology of the signal, can be seen between the blue and red wavelengths (Pearson correlation coefficient = –0.565). (b) The similarity between both the timing and morphology of the signal can be seen between blue and green wavelengths (Pearson correlation coefficient = 0.999).

between blue and red, but not between the blue and green signals (Fig. 4), as noted by the correlation coefficients between the signals.

From these plots, it can be seen that the primary source of signal generation for the shorter wavelengths is similar, while the source of signal generation is different for the red wavelength. To confirm that higher absorbance of blood at short wavelengths drives the signal generation, comparison of the flow in the vasculature was performed with the optofluidic phantom system, which mimics the flow through the small intestine.[26] While a comparison of the flow velocity through the cranial mesenteric artery to the optical signals would be ideal, it is difficult to correctly match pulses between the artery and the sensor, given the unknown vascular path length between the two points. The use of the *in vitro* system provided a defined path of fluid flow and a more reliable comparison of the flow to

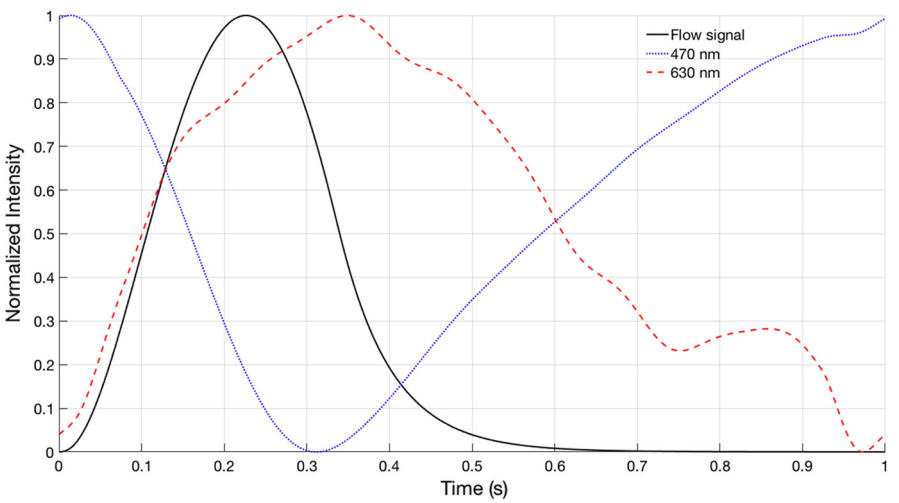

Fig. 5 Optical signal changes in response to oxygenated blood phantom flowing through the intestinal phantom. For the shorter wavelengths, increased flow to the tissue results in reduced signal intensity returning to the detector. This trend is reversed for the longer wavelengths, where absorption does not dominate.

the optical signals. The optical signals generated from the phantom are depicted in Fig. 5 and are plotted alongside one cycle of pump flow signal flowing through the phantom. A pulsed pump flow waveform, as shown in Fig. 5, was used to represent the vascular flow entering the capillary bed.

As can be seen in Fig. 5, the decrease in the blue signal follows the increase in flow, while the red signal can be seen to increase following the increase in flow. These results match what was observed *in vivo* and indicate that for shorter wavelengths, where absorbance is high, light attenuation is the dominant source of signal generation, while the dominant source for longer wavelengths, where the ratio of the scattering coefficient to the absorption coefficient is greater, comes from the effects discussed above. From these results, perfusion of the intestinal tissue can be optically measured through the alterations in pulsatile amplitude for signals being primarily modulated by the attenuation of light through absorbance or through the monitoring of nonpulsatile changes across the spectrum of wavelengths. Decreases in pulsatile amplitudes here can be seen as decreases in perfusion through occlusion of the vessel. This is seen most clearly in the shorter wavelength data. The multiple changes observed in the nonpulsatile signals among the three wavelengths lead to the possibility that changes in perfusion and oxygenation can be differentiated, which is further explored below.

3.2 *Hypoxia*

Estimation of the oxygenation of the jejunum tissue was first performed utilizing the method applied in commercial pulse oximeters, namely, the modulation ratio (R). Figures 6(a) and 6(b) depict the modulation ratios from both the red–blue and green–blue sensors, plotted along with the systemic SpO_2. The systemic SpO_2 was determined using the commercial pulse oximeter placed on the tongue for both rabbit 1 and rabbit 2 during the hypoxia episodes. Although shorter wavelengths are used to minimize penetration depth, the intestinal tissue remains relatively thin (~2 mm) and, as a result, the modulation ratio, R, is very susceptible to noise from slight movements. As depicted in the figure, due to the noise, a strong relationship between R and the systemic SpO_2 is not apparent, across animals or across (red/blue and green/blue) sensors.

To overcome the poor correlations seen using the conventional R parameter, due to the additional environmental noise component, a method using the Pearson correlation coefficient was developed and tested as a measure for oxygenation. The method calculates the Pearson correlation coefficient between the averaged pulsatile waveforms for each wavelength over sequential time segments. This method derives its efficacy from the shift in the ratio of the effects leading to the generation of the pulsatile signal for the red wavelength. It was determined that as oxygenation decreased, the red and blue signals became closer in phase, resulting in an increased correlation. The phase difference between green and blue did not represent changes in oxygenation very well. As illustrated in Figs. 6(c) and 6(d), this method showed improved correlations with changes in systemic SpO_2 in both rabbits for the blue/red signal. To relate this figure with actual intestinal oxygenation, a calibration would need to be performed, since this value may differ from systemic oxygenation. Using the blue/green sensor and calculating this correlation figure yielded a highly correlated signal, since the phase difference between green and blue poorly represented changes in oxygenation.

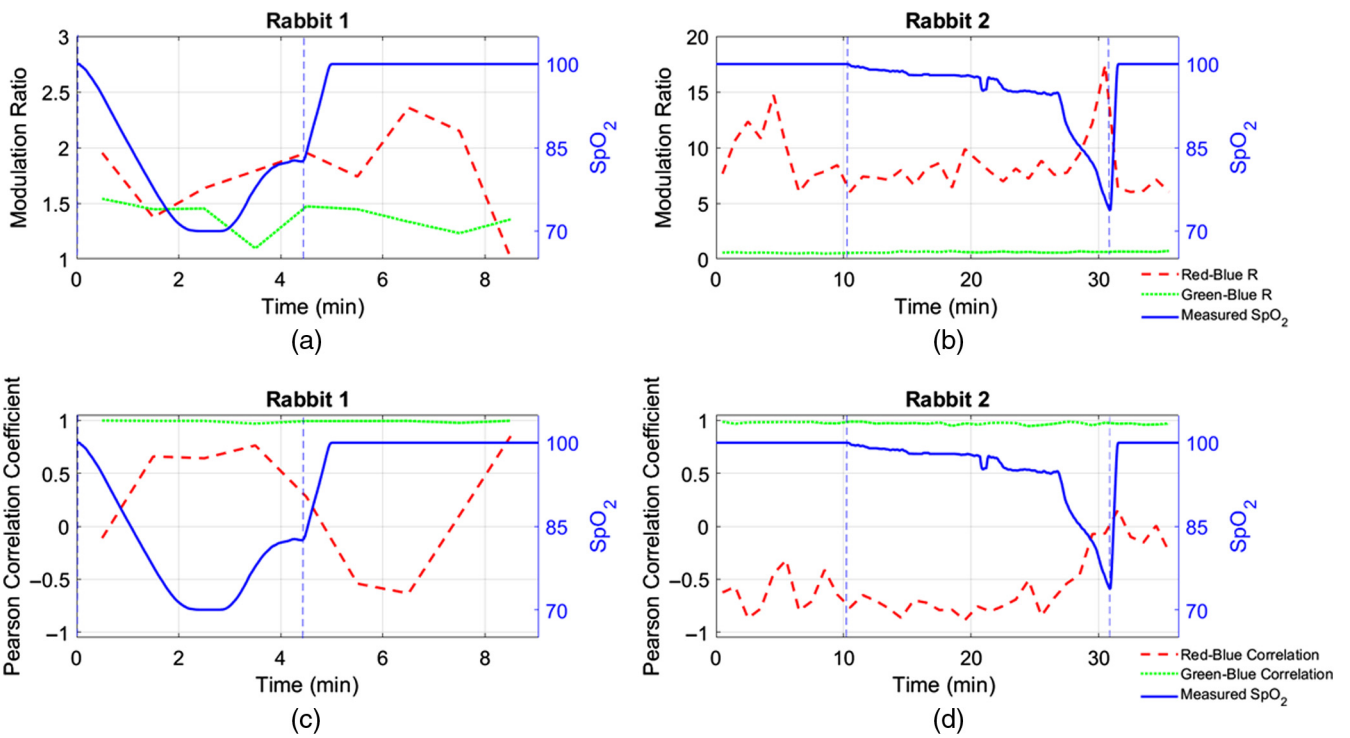

Fig. 6 Modulation ratios and systemic SpO_2 versus time during the hypoxia episode for (a) rabbit 1 and (b) rabbit 2. Correlation coefficients between wavelengths on each sensor and the systemic SpO_2 plotted over time during the hypoxia episode for (c) rabbit 1 and (d) rabbit 2. Vertical dashed lines indicate the beginning and end of the hypoxic period.

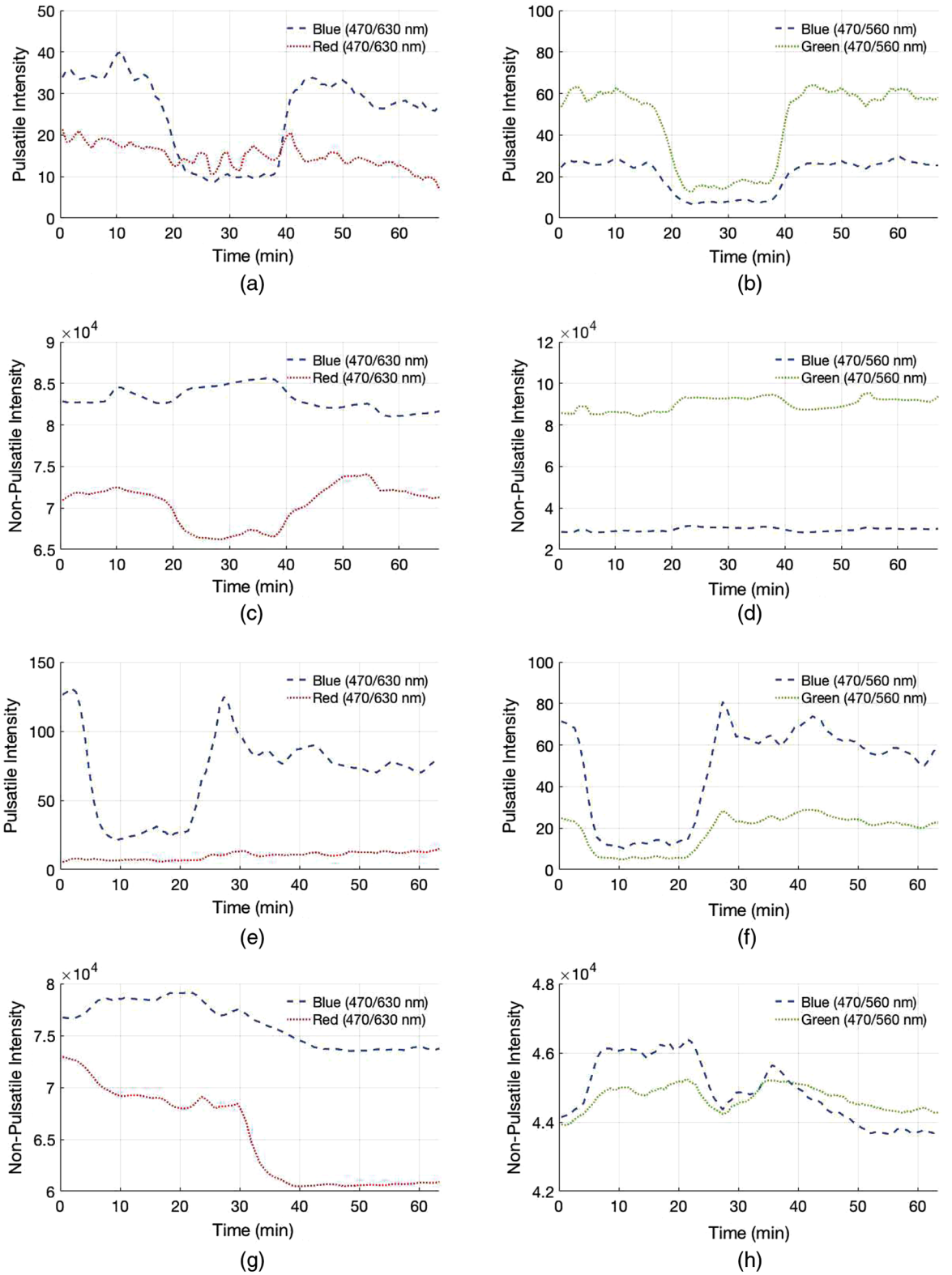

Fig. 7 Changes in response to hemorrhagic shock for (a–d) rabbit 1 and (e–h) rabbit 3 of the pulsatile components of the blue and red sensor (a,e), the pulsatile components of the blue and green sensor (b,f), the nonpulsatile components of blue and red sensor (c,g) and the nonpulsatile components of the blue and green sensor (d,h). The amplitude of the pulsatile components of the blue and green signals across both sensors can be seen to generally decrease during the shock segment (8 to 23 min) and return to near baseline during the recovery segment (25 to 60 min). There was a slight drop after initial recovery at 28 min as excess fluid was added between 28 and 33 min (especially noticeable in the blue pulsatile signal on both sensors and to a lesser extent on the green pulsatile signal). For the nonpulsatile signals, the blue and green signals increased slightly during shock and the red signal decreased slightly while all three nonpulsatile signals decreased upon recovery.

3.3 *Hemorrhagic Shock*

Utilizing the analysis discussed above, perfusion and blood oxygenation changes in the small intestine were examined during hemorrhagic shock. Time-domain comparisons of the signals can be seen in Fig. 7. For rabbit 1 (a–d), the initial segment of the data before the removal of blood spans from 0 to 18 min, the shock segment when blood was removed spans from 23 to 38 min, and the recovery segment after blood was returned spans from 42 to 68 min. For rabbit 3 (e–h), the initial segment of the data before the removal of blood spans from 0 to 5 min, the shock segment from 8 to 23 min, and the recovery segment from 25 to 60 min.

From the above plots, the trends observed in the perfusion study for the different wavelengths are also observed in the shock data. With decreases in overall flow to the intestine, occurring via hypovolemia, in this case, the nonpulsatile components of the signals change similarly to those in the perfusion study. Specifically, decreased flow leads to increases in the amplitude of the shorter wavelength signals and decreases in the amplitude of the longer wavelength signal. The blue and green pulsatile signals also decreased in amplitude during shock but the red pulsatile signal did not show sensitivity to this condition. The addition of excess fluid in the recovery segment introduced further changes to signal intensities. The difference in sensor placement for the 470/630 nm sensor and 470/560 nm sensor introduced slight differences in the observed signals due to the different vascular beds probed. This is more evident in the observed nonpulsatile changes, where the blue signal intensity is more pronounced and shows a different time course upon recovery for one of the sensors as compared to the other. Since local physiological controls within the small intestine play a dominate role in maintaining intraorgan pressure and hemodynamics compared to the influence of the central nervous system, the differences between the signals may be attributed to differences in local hemodynamics.[36] Oxygenation information is also present in these signals and is assumed to be present in this study, because oxygen debt is known to accrue during ischemia.[37] While the level of oxygen debt and interorgan compensation varies among hemorrhagic shock cases, because the animals were bled until they reached half pressure and maintained there over a significant period of time, a shift in tissue oxygenation is possible during the protocol carried out in this study. Depicted in Fig. 8 are the Pearson correlation coefficients of the signals during the shock episodes. The timing for this shock data is the same as described for Fig. 7, but the data shown are for (a) rabbit 1 and (b) rabbit 3.

Although there are differences between the two rabbits, similar features can be observed. Increases in the correlation coefficient can be seen during the shock segment, showing the effects of both the perfusion and oxygenation changes. A feature in which these two plots differ is the new baseline reached during the recovery period with respect to the original baseline. In the case of rabbit 1, the final value is greater than the initial, while in the case of rabbit 3, this observation is reversed. The increased value observed during the recovery period may be due to oxygen debt accumulated during the shock segment. While this was not observed in both rabbits, in rabbit 1, where this was seen, blood flow through the cranial mesenteric artery was measured and shown to be reduced, as compared to rabbit 3 during all parts of the specimen's procedure. Specifically, the average flow rate in rabbit 1 was 30 ml/min as compared to 120 ml/min in rabbit 3. Hemorrhage generally results in the shunting of blood away from the peripheral (and visceral) organs and distributing the blood to vital organs preferentially. Reduced flow despite resuscitation to the intestine can be interpreted as a continuation of a survival response that was already in progress. This perfusion difference could be seen to contribute to the difference in the response of the tissue to the hypovolemic insult. Observing such "patient-specific" responses by

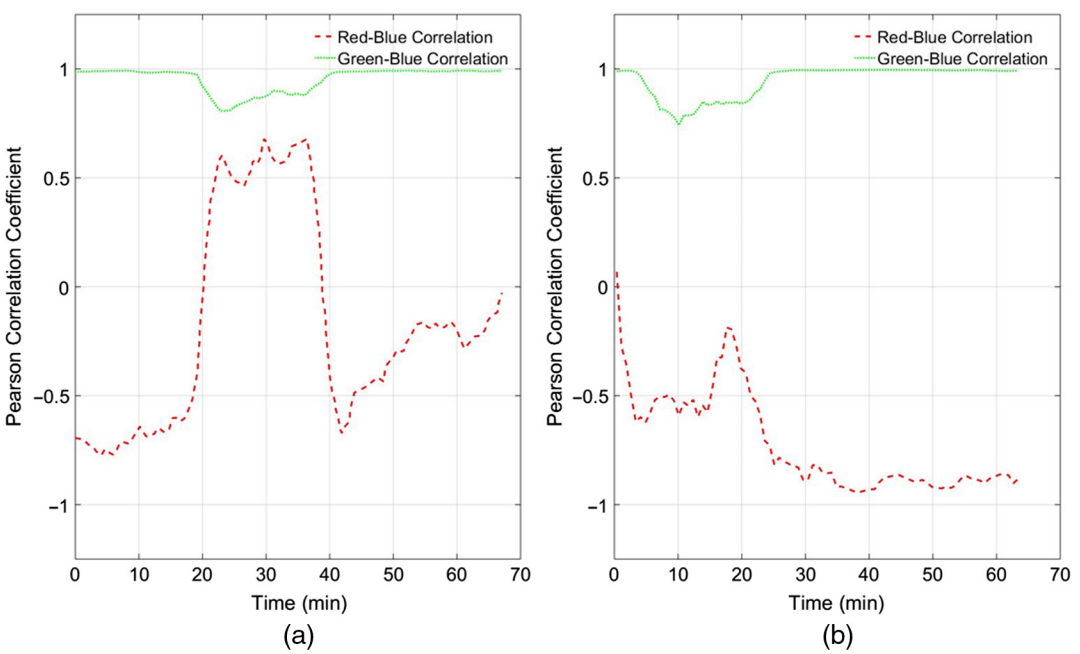

Fig. 8 Plots of the Pearson correlation coefficient between the red and blue signals for (a) rabbit 1 and (b) rabbit 3.

using this type of monitor may provide an important tool in determining optimal resuscitation protocols.

Hemorrhagic shock associated with traumatic injury may be related to extremity, thoracic or abdominal sources. Abdominal injuries are often associated with significant hemorrhagic shock. For this subset of patients, two operations are often performed: an initial operation to stop hemorrhage and a subsequent procedure within 2 days for definitive reconstruction of injured tissue. During the intervening time between the procedures, resuscitation is typically performed. This clinical care model enables implantation of a sensor on intestinal tissue at the initial operation, use of the sensor to direct resuscitation, and then removal at the time of the second operation. As such, risks of chronic implantation are avoided while providing the benefits of monitoring a key tissue site.

4 Conclusion

In this research, two sensors were developed that collectively utilized three optical wavelengths (470, 560, and 630 nm) to specifically assess changes in perfusion and oxygenation in the small intestine *in vivo*. Using vessel occlusion, systemic changes in oxygenation input, and induction of hemorrhagic shock, the capabilities and sensitivity of the sensor were explored using the three wavelengths. Analysis of the PPG data was performed using a Pearson correlation coefficient algorithm. The conventional modulation ratio method was ineffective at tracking oxygenation in the presence of noise due to motion and the variability introduced by the morphology of the intestine. Hence, an algorithm was introduced. The method utilized the difference in phase between two different wavelength signals to assess oxygen content. Pulsatile and nonpulsatile components of the red, blue, and green wavelength signals were analyzed for all three protocols (occlusion, systemic oxygenation changes, and shock) and were shown to differentiate perfusion and oxygenation changes in the jejunum. The blue and green signals produced better correlations for perfusion changes during occlusion and shock, while the red and blue signal, using a new correlation algorithm, showed better results for assessing changes in oxygenation induced systemically and locally during shock.

Disclosures

The authors have no financial interests or potential conflict of interest to disclose concerning this work.

Acknowledgments

The authors acknowledge the support from the National Institutes of Health under Grant No. 1 R21 EB020398. A.M. W. thanks the Texas A&M University Graduate Diversity Fellowship Program.

References

1. P. C. Spinella and J. B. Holcomb, "Resuscitation and transfusion principles for traumatic hemorrhagic shock," *Blood Rev.* **23**(6), 231–240 (2009).
2. E. E. Fox et al., "Earlier endpoints are required for hemorrhagic shock trials among severely injured patients," *Shock* **47**(5), 567–573 (2017).
3. C. Fries and M. J. Midwinter, "Trauma resuscitation and damage control surgery," *Surgery* **28**(11), 563–567 (2010).
4. S. A. Tisherman et al., "Clinical practice guideline: endpoints of resuscitation," *J. Trauma* **57**(4), 898–912 (2004).
5. G. Tachon et al., "Microcirculatory alterations in traumatic hemorrhagic shock," *Crit. Care Med.* **42**(6), 1433–1441 (2014).
6. E. A. Deitch, "Multiple organ failure. Pathophysiology and potential future therapy," *Ann. Surg.* **216**(2), 117–134 (1992).
7. S. K. Shah et al., "Resuscitation-induced intestinal edema and related dysfunction: state of the science," *J. Surg. Res.* **166**(1), 120–130 (2011).
8. L. S. L. Arakaki et al., "Muscle oxygenation as an early predictor of shock severity in trauma patients," *Shock* **47**(5), 599–605 (2017).
9. M. Wilson, D. P. Davis, and R. Coimbra, "Diagnosis and monitoring of hemorrhagic shock during the initial resuscitation of multiple trauma patients: a review," *J. Emerg. Med.* **24**(4), 413–422 (2003).
10. J. W. Kern and W. C. Shoemaker, "Meta-analysis of hemodynamic optimization in high-risk patients," *Crit. Care Med.* **30**(8), 1686–1692 (2002).
11. F. A. Moore et al., "Inflammation and the host response to injury, a large-scale collaborative project: patient-oriented research core–standard operating procedures for clinical care. III. Guidelines for shock resuscitation," *J. Trauma* **61**(1), 82–89 (2006).
12. L. Paladino et al., "The utility of base deficit and arterial lactate in differentiating major from minor injury in trauma patients with normal vital signs," *Resuscitation* **77**(3), 363–368 (2008).
13. B. A. McKinley et al., "Tissue hemoglobin O_2 saturation during resuscitation of traumatic shock monitored using near infrared spectrometry," *J. Trauma* **48**(4), 637–642 (2000).
14. L. N. Diebel et al., "Effect of acute hemodilution on intestinal perfusion and intramucosal pH after shock," *J. Trauma* **49**(5), 800–805 (2000).
15. S. M. Cohn et al., "Tissue oxygen saturation predicts the development of organ dysfunction during traumatic shock resuscitation," *J. Trauma* **62**(1), 44–54, discussion 54–55 (2007).
16. C. Y. Wu et al., "Effects of different types of fluid resuscitation for hemorrhagic shock on splanchnic organ microcirculation and renal reactive oxygen species formation," *Crit. Care* **19**, 434 (2015).
17. B. Zingarelli and J. M. Kaplan, "What's new in shock, May 2017?" *Shock* **47**(5), 533–536 (2017).
18. Nellcor technical staff, "A technology overview of the nellcor oximax pulse oximetry system," Medtronic/Covidien, Colorado, https://pdfs.semanticscholar.org/3220/449d97994890bc19c9dd526da2124455fb97.pdf (2003).
19. A. Plüddemann et al., "Pulse oximetry in primary care: primary care diagnostic technology update," *Br. J. Gen. Pract.* **61**(586), 358–359 (2011).
20. Y. Mendelson, R. J. Duckworth, and G. Comtois, "A wearable reflectance pulse oximeter for remote physiological monitoring," in *Proc. of Int. Conf. of the IEEE Engineering in Medicine and Biological Society*, pp. 912–915, IEEE (2006).
21. Y. Shimada et al., "Evaluation of a new reflectance pulse oximeter for clinical applications," *Med. Biol. Eng. Comput.* **29**(5), 557–561 (1991).
22. T. J. Akl et al., "Intestinal perfusion monitoring using photoplethysmography," *J. Biomed. Opt.* **18**(8), 087005 (2013).
23. C. G. Cronin et al., "Normal small bowel wall characteristics on MR enterography," *Eur. J. Radiol.* **75**(2), 207–211 (2010).
24. D. A. Boas, C. Pitris, and N. Ramanujam, Eds., *Handbook of Biomedical Optics*, CRC Press, Taylor and Francis Group, Boca Raton, Florida (2012).
25. S. Prahl, "Optical absorption of hemoglobin," Oregon Medical Laser Center, https://omlc.org/spectra/hemoglobin/index.html (1999).
26. M. B. Robinson et al., "In-silico and in-vitro investigation of a photonic monitor for intestinal perfusion and oxygenation," *Biomed. Opt. Express* **8**(8), 3714–3734 (2017).
27. K. J. Brasel, "Advanced trauma life support (ATLS(R)): the ninth edition," *J. Trauma Acute Care Surg.* **74**(5), 1363–1366 (2013).
28. S. A. Skinner and P. E. O'Brien, "The microvascular structure of the normal colon in rats and humans," *J. Surg. Res.* **61**(2), 482–490 (1996).
29. A. P. Lima, P. Beelen, and J. Bakker, "Use of a peripheral perfusion index derived from the pulse oximetry signal as a noninvasive indicator of perfusion," *Crit. Care Med.* **30**(6), 1210–1213 (2002).
30. P. D. Mannheimer, "The light-tissue interaction of pulse oximetry," *Anesth. Analg.* **105**(6 Suppl.), S10–S17 (2007).
31. J. G. Webster, *Design of Pulse Oximeters*, Institute of Physics Publ., Bristol, Pennsylvania (1997).
32. J. A. Nijboer, J. C. Dorlas, and H. F. Mahieu, "Photoelectric plethysmography—some fundamental aspects of the reflection and transmission method," *Clin. Phys. Physiol. Meas.* **2**(3), 205–215 (1981).

33. J. Weinman, A. Hayat, and G. Raviv, "Reflection photoplethysmography of arterial-blood-volume pulses," *Med. Biol. Eng. Comput.* **15**(1), 22–31 (1977).
34. A. A. Kamshilin and N. B. Margaryants, "Origin of photoplethysmographic waveform at green light," *Phys. Proc.* **86**, 72–80 (2017).
35. A. A. Kamshilin et al., "A new look at the essence of the imaging photoplethysmography," *Sci. Rep.* **5**, 10494 (2015).
36. U. Haglund and D. Bergqvist, "Intestinal ischemia—the basics," *Langenbecks Arch. Surg.* **384**(3), 233–238 (1999).
37. P. J. Matheson, M. A. Wilson, and R. N. Garrison, "Regulation of intestinal blood flow," *J. Surg. Res.* **93**(1), 182–196 (2000).

Biographies for the authors are not available